European Journal of Oral Sciences

Eur J Oral Sci 2019; 127: 112–121
DOI: 10.1111/eos.12594
Printed in Singapore. All rights reserved

© 2018 Eur J Oral Sci
European Journal of Oral Sciences

Proteomic analysis of dentin–enamel junction and adjacent protein-containing enamel matrix layer of healthy human molar teeth

Michal Jágr[1,2], Peter Ergang[1], Statis Pataridis[1], Marta Kolrosová[3], Martin Bartoš[4], Ivan Miksík[1]
[1]Institute of Physiology, The Czech Academy of Sciences, Prague; [2]Quality of Plant Products, Crop Research Institute, Prague; [3]Department of Analytical Chemistry, Faculty of Science, Charles University, Prague; [4]Institute of Dental Medicine, First Faculty of Medicine, Charles University and General University Hospital, Prague, Czech Republic

Jágr M, Ergang P, Pataridis S, Kolrosová M, Bartoš M, Mikšík I. Proteomic analysis of dentin–enamel junction and adjacent protein-containing enamel matrix layer of healthy human molar teeth.
Eur J Oral Sci 2019; 127: 112–121. © 2018 Eur J Oral Sci

The dentin–enamel junction (DEJ) is the border where two different mineralized structures – enamel and dentin – meet. The protein-rich DEJ, together with the inner enamel region of mature teeth, is known to exhibit higher fracture toughness and crack growth resistance than bulk phase enamel. However, an explanation for this behavior has been hampered by the lack of compositional information for the DEJ and the adjacent enamel organic matrix (EOM). We studied proteomes of the DEJ and EOM of healthy human molars and compared them with dentin and enamel proteomes from the same teeth. These tissues were cut out of tooth sections by laser capture microdissection, proteins were extracted and cleaved by trypsin, then processed by liquid chromatography coupled to tandem mass spectrometry to analyze the proteome profiles of these tissues. This study identified 46 proteins in DEJ and EOM. The proteins identified have a variety of functions, including calcium ion-binding, formation of extracellular matrix, formation of cytoskeleton, cytoskeletal protein binding, cell adhesion, and transport. Collagens were identified as the most dominant proteins. Tissue-specific proteins, such as ameloblastin and amelogenin, were also detected. Our findings reveal new insight into proteomics of DEJ and EOM, highly mineralized tissues that are obviously difficult to analyze.

Michal Jágr, Institute of Physiology, The Czech Academy of Sciences, v.v.i., Vídeňská 1083, 14220 Prague 4, Czech Republic

E-mail: Michal.Jagr@fgu.cas.cz

Key words: dentin; laser capture microdissection; mass spectrometry; proteome

Accepted for publication October 2018

Teeth are remarkably successful natural bioceramic composite structures. They are composed of two unique tissues: a hard outer layer of enamel, which resists wear and acid attack; and dentin, which is a resilient internal layer, more flexible than enamel, that provides fracture resistance.

Mature enamel is a brittle material composed predominantly of carbonated calcium hydroxyapatite (96%) with 3% water and 1% organic matrix (1). A series of programed physiological and chemical events are involved in enamel formation, including gene expression, protein secretion, protein folding and assembly, mineral growth, and protein degradation. The extracellular matrix is continuously secreted during enamel formation, resulting in production of mineralized matrix. The composition of the matrix varies during the different stages of enamel mineralization, with the matrix being rapidly degraded during the maturation stage (when crystals grow mainly in width and thickness), eventually being removed from the extracellular space to allow completion of mineralization (2). During maturation, massive protein-degradation events occur simultaneously with the completion of mineralization. These extracellular events transform matrix, which contains approximately 30% mineral by weight – the remainder being water and organic material – into a highly organized structure that is almost completely inorganic (3).

In contrast to enamel, tooth dentin is a collagenous tissue that is traversed by dentinal tubules containing cytoplasmic extensions of odontoblasts. It is a highly mineralized tissue that forms the bulk of the tooth, serving as a protective covering for the pulp as well as a support for overlying enamel. In our previous studies, we analyzed proteomics of human tooth dentin and pulp (4, 5). We detected 140 (pulp/dentin) shared proteins, 37 of which were not observed in plasma. We suggested that these proteins might participate in the unique pulp–dentin complex (5). On a weight basis, mature dentin consists of approximately 70% mineral, 20% organic matrix, and 10% water (6, 7).

Interfaces between two dissimilar materials, such as enamel and dentin, usually concentrate stresses and enamel can delaminate. However, the dentin–enamel junction (DEJ) is remarkably successful in transferring applied loads from enamel to dentin (8). The DEJ is a

complex and (until now) poorly defined structure, which bridges enamel to the bulk of dentin. It can be seen on sections as a scalloped line between the two mineralized structures (9). Despite a human lifetime of repeated masticatory, parafunctional, and occasional impact loadings, enamel rarely separates from dentin. Furthermore, the DEJ is highly damage tolerant. Cracks that initiate in enamel are often deflected or limited by the DEJ. Hence, most cracks do not continue to propagate into dentin and through the entire tooth (10). It has been proposed that the crack-resistance of the DEJ may originate from a gradation of mechanical properties and the unique protein composition of this layer (10). The DEJ interface is thought to represent the original position of the basement membrane of ameloblasts and odontoblasts when they are in contact in the embryological tooth bud. When biomineralization starts, ameloblasts and odontoblasts move away from each other in opposite directions, leaving protein-rich matrices in their respective wakes. These protein-rich matrices guide mineralization. Thus, this optically distinct line is usually thought to represent an abrupt demarcation between these matrices (10). The DEJ constitutes a biomimetic model of a structure uniting dissimilar materials with a special mix of proteins, which may define the unique properties of the DEJ. Its composition includes collagen type I, phosphorylated and non-phosphorylated proteins (e.g. small leucine-rich proteoglycans), and some extracellular matrix molecules originating from blood serum. Enzymes, metalloproteinases, and lipoproteins participate in DEJ formation (11).

Although the extracellular organic matrix of enamel is largely removed during enamel maturation, a small amount of protein (~1% wt) remains in enamel that forms the enamel organic matrix (EOM), namely proteolyzed fragments and an insoluble protein matrix distributed along the dentinal surface (10, 12). The EOM layer is the post-eruptive tissue of enamel that begins at the dentin DEJ and extends 100–400 μm toward the outer tooth surface (13). The relatively higher content of proteins, together with less mineralization of the enamel region closest to the thin DEJ layer, is believed to toughen the inner enamel region and/or fills and stops cracks formed within enamel (14). The EOM, together with proteins in the DEJ, can be defined as an interphase region of functionally graded properties, intermediate between those of bulk phase enamel and those of dentine.

Laser capture microdissection (LCM) has helped develop a high-end research and diagnostic technique suitable for obtaining well-defined samples of precise tissue areas for widespread genomic and proteomic analyses. This method facilitates isolation of a pure population of cells and tissues without an admixture of various unintentional cells, simply by eliminating the heterogeneous background. The LCM system represents a modified microscopic technique and allows selection of cells within histological sections and their contact-free laser-mediated catapult into a test tube. The LCM-dissected tissues are subjected to protein extraction, reduction, alkylation, and digestion, followed by injection into a nano-liquid chromatography coupled to tandem mass spectrometry (nLC-MS/MS) system for chromatographic analysis and protein identification (15–17).

Applications of LCM for the study of various oral tissues have been reported in many recent investigations. Laser capture microdissection was used for expression analysis of human salivary glands and differences between submandibular and labial glands were detected (18). The common research of highly mineralized tooth tissues is fraught with difficulties in preparing intact, unfixed, undecalcified sections of highly mineralized tissues, such as dentin, tooth cementum, and enamel. A modified procedure of sectioning unfixed and undecalcified frozen mouse mandibles was described to have been used for dental hard tissue-associated cells (19). More recently, use of LCM in oral biosciences has been thoroughly reviewed in a study by Thennavan *et al*. (20).

The main aim of this study was to identify proteins in the precise structures of the DEJ and the surrounding EOM and to compare them with the proteins of mature enamel and dentin tissues obtained from healthy human third molars. To the best of our knowledge, no study using LCM to investigate the DEJ and EOM proteome has been presented until now.

Material and methods

Chemicals

Trypsin [tosyl phenylalanyl chloromethyl ketone (TPCK)-treated from bovine pancreas, 13,500 units per mg], ammonium bicarbonate, 2,2,2-trifluoroethanol (TFE), dithiothreitol (DTT), and iodoacetic acid were obtained from Sigma (St Louis, MO, USA). Acetonitrile LC-MS Ultra Chromasolv and formic acid for mass spectrometry came from Sigma. All solutions were prepared in MilliQ water (Millipore, Bedford, MA, USA).

Sample preparation

Healthy and completely erupted permanent human third molars with closed apexes ($n = 6$) were extracted for various clinical reasons from adults of ages 18–24 yr; both genders were represented equally. Some teeth were extracted because of their anomalous positions (mesial or distal inclination) or because of difficulties associated with the process of their eruption. All teeth were extracted in a dental clinic after acquiring patients' informed consent regarding donation of teeth for research and in accordance with The Code of Ethics of the World Medical Association for experiments involving humans.

The teeth were washed thoroughly with water, then cementum and soft tissues were mechanically scraped off with an iron spatula and the teeth were cleaned with brushes. Each tooth was then cut horizontally (below the level of enamel) and only the upper part (the crown) was used for the experiment. The crowns were subsequently cut into two sections, ~ 1-mm-thick, using a high-speed drill (Dremel, Racine, WI, USA) with continual cooling with water. Then each section was ground to a thickness of ~ 70–100 μm. All sections were washed with water and stored at −80°C for further processing.

Laser capture microdissection

The ground sections of teeth were mounted with TissueTek glue (Sakura Finetek, AJ Alphen aan den Rijn, the Netherlands) onto microscopic slides coated with polyethylene naphthalene membrane (FrameSlides PET membrane 1.4 mm; cat. no. 11505151; Leica Microsystems, Wetzlar, Germany), and specific areas representing dentin, enamel, and DEJ with surrounding EOM (for details see Fig. 1) were dissected using an LMD6000 Laser Capture Microdissection Microscope System (Leica Microsystems) with 100 mW semiconductor blue pulse laser at 130% power. We used the hand-guiding mode for cutting. The dissected areas were ~ 40,000–200,000 μm^2 for each sample. The collection tube contained 20 μl of pure water to minimize electrostatic interactions. Six teeth were used for the preparation of, in total, 12 tooth sections (two sections from each tooth). Two samples of dentin, two samples of DEJ + EOM, and two samples of enamel were taken from each tooth section. This means that there were 72 samples in total (24 samples of each tooth tissue type, namely enamel, dentin, and DEJ with surrounding EOM).

The microdissected samples were captured into caps of the microcentrifuge tubes and then immediately transferred into glass vials for further treatment.

Protein preparation and trypsin digestion

Two protein-extraction methods were used in this study, and all 72 samples were divided equally into two groups of 36 samples subjected to each protein-extraction method.

For the first extraction method (Method 1), the LCM samples were swollen in 100 μl of 50 mM ammonium bicarbonate, then heated at 105°C for 5 min. After cooling to room temperature, 2 μl of trypsin-containing digestion solution (50 mM ammonium bicarbonate, with trypsin at a concentration 0.1 mg ml^{-1}) was added and samples were incubated at 37°C overnight. The next day, this process (addition of 100 μl of 50 mM ammonium bicarbonate, heating to 105°C for 5 min, and incubation with 2 μl of digestion solution containing trypsin) was repeated once again (overnight at 37°C).

The second extraction method (Method 2) was adapted from a published protocol (16). Briefly, 200 μl of a mixture of 50 mM ammonium bicarbonate with TFE (1:1, v/v) was added to a vial containing an LCM sample to initiate protein extraction. The vial was incubated for 15 min at 90°C and vortexed several times. Supernatant was concentrated to 10 μl using a vacuum concentrator and then transferred to a glass vial. In the next step, 1 μl of 100 mM DTT was added to the solution and incubated for 15 min at 80°C to reduce the cysteine residues. Incubation was carried out for 30 min at room temperature. In the next step, 1 μl of 200 mM iodoacetamide was added to the solution and left for 30 min in the dark and at room temperature. Finally, 45 μl of 50 mM ammonium bicarbonate was added, as well as 100 ng of trypsin. Incubation was carried out with gentle mixing, using a thermomixer, overnight at 37°C. Samples were treated with maximal care to ensure minimal keratin contamination.

Finally, all the trypsin digests from both extraction methods were processed using Stage Tips, C18 Empore SPE Disks from Sigma (21). The resulting extracts were concentrated in a vacuum centrifuge to dry out. Dried extracts were stored at −80°C before analysis.

Analysis of peptide digests with nLC-MS/MS, and protein identification

Dried protein digests were dissolved in 20 μl of 1% formic acid, centrifuged, and the supernatant was transferred to inserts in vials.

The nano-LC apparatus used for analysis of protein digests was Proxeon Easy-nLC (Proxeon, Odense, Denmark) coupled to a MaXis Q-TOF (quadrupole–time of flight) mass spectrometer with ultra-high resolution (Bruker Daltonics, Bremen, Germany) by a nanoelectrosprayer. The nLC-MS/MS instruments were controlled with software

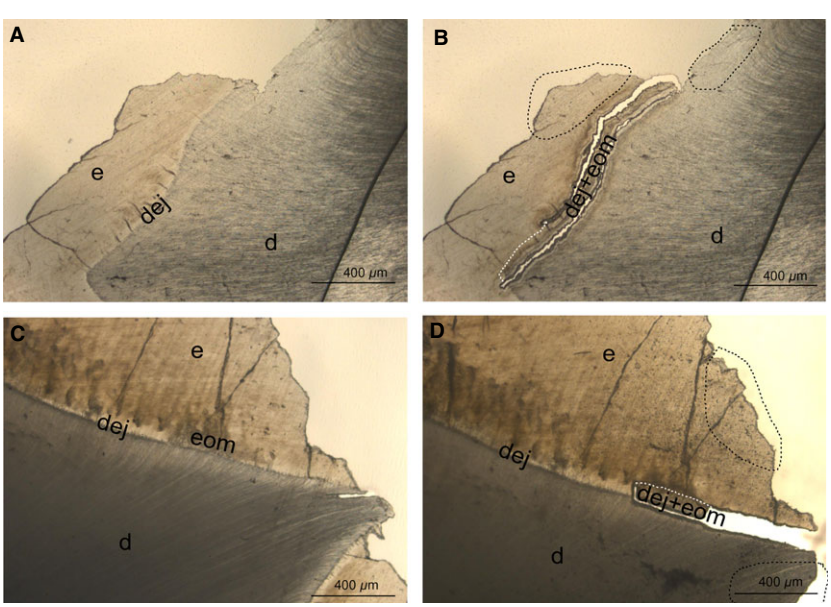

Fig. 1. Photographs of tooth sections obtained from a laser microdissection microscope. (A, C) View before laser microdissection of the tooth samples. (B, D) The same sections as in A and C, respectively, after procession. d, dentin; dej, dentin-enamel junction; e, enamel; eom, enamel organic matrix. Scale bars = 400 μm. Dotted areas indicate the area where the enamel, dentin–enamel junction, and dentin samples were taken.

packages HYSTAR 3.2 and OTOFCONTROL 3.4 (Bruker Daltonics). Data were collected and analyzed using software packages PROTEINSCAPE 3.0.0.446 and DATAANALYSIS 4.2 (Bruker Daltonics). Ten microliters of peptide mixture was injected into an NS-AC-12-dp3 BioSphere C18 column (particle size, 3 μm, pore size, 12 nm, length, 200 mm, inner diameter, 75 μm) that contained an NS-MP-10 BioSphere C18 pre-column (particle size: 5 μm, pore size: 12 nm, length: 20 mm, inner diameter: 100 μm), both obtained from NanoSeparations (Nieuwkoop, the Netherlands).

Separation of peptides was achieved via a linear gradient between mobile phase A (water) and mobile phase B (acetonitrile), both containing 0.1% (v/v) formic acid. The separation was started with gradient elution from 5% to 7% mobile phase B in 5 min, followed by gradient elution to 30% mobile phase B at 180 min. The next step was gradient elution to 50% mobile phase B in 10 min, and then a gradient to 100% mobile phase B in 10 min was used. Finally, the column was eluted with 100% mobile phase B for 20 min. Equilibration before the subsequent run was achieved by washing the column with 3 μl of 5% mobile phase B for 5 min. The flow rate was 0.2 μl min^{-1}, and the column was held at ambient temperature (25°C).

Online nano-electrospray ionization (easy nano-ESI) in the positive mode was used. The ESI voltage was set at +4.5 kV with spectra rate 3 Hz. Operating conditions were: drying gas (N_2), 4 l min^{-1}; drying gas temperature, 180°C; and nebulizer pressure, 100 kPa. Experiments were performed by scanning from 50 to 2,200 mass-to-charge ratio (m/z). The reference ion used (internal mass lock) was a monocharged ion of $C_{24}H_{19}F_{36}N_3O_6P_3$ (m/z = 1221.9906). For MS/MS analyses, auto MS/MS with active exclusion (after 1 spectrum and release after 0.3 min) was set on. All LC-MS/MS analyses were performed in duplicate as in the previous study (22). Data were processed using PROTEINSCAPE software (ver. 3.0.0.446). Proteins were identified by correlating tandem mass spectra to the UniProt human database using the MASCOT search engine (ver. 2.3.0, www.matrixscience.com). Database searches were performed, as described in our previous study, with the taxonomy restricted to *Homo sapiens* to remove protein identification redundancy (23). Briefly, trypsin (or semitrypsin) was chosen as an enzyme parameter. Three missed cleavages were allowed, and an initial peptide mass tolerance of ±15.0 ppm was used for MS analysis and of ±0.03 Da for MS/MS analysis. The following variable modifications were considered: carbamidomethylation of cysteine; carboxymethylation of cysteine; oxidation of methionine; and hydroxylation of lysine and proline. Only significant hits (MASCOT score of ≥ 80 for proteins) were accepted. The Peptide Decoy option was selected during the data-search process to remove false-positive results.

Statistics

Cluster analysis was used to identify differences in protein composition between the dental tissues (DEJ + EOM, enamel and dentin) of individual samples investigated with respect to their gender and biological variation.

Results

Tooth sections were obtained from healthy third-molar teeth (n = 6). Two sections were prepared from each tooth. Each section was used for preparation of six micro-samples by LCM (two samples of dentin, two samples of DEJ + EOM, and two samples of enamel) (Fig. 1). The total number of samples was 72. We observed that the tooth sections did not need to be demineralized before LCM for distinct sections of DEJ + EOM, enamel, and dentin to be cut. Repeated laser cutting with prolonged time was successful in cutting samples of area 40,000–200,000 μm^2. The samples were randomized and processed as described in the Material and methods. Proteins were extracted using two different and independent methods. Most proteins were extracted by both methods, but some proteins could be detected only when extracted using one of the two methods. Thus, use of two different extraction methods was able to expand the list of proteins detected in samples of DEJ + EOM, enamel, and dentin.

A total of 46 proteins were detected in DEJ + EOM samples (Table 1, Table S1). These proteins have a variety of functions. Their functions in biological processes were categorized according to the classification system used in the public database (available at http://www.hprd.org). The majority of the proteins identified in our research (Figs 2 and 3) were mainly involved in cell growth and/or in the maintenance of DEJ + EOM (37.0%). Other, most significant, functions were cell communication and signal transduction (23.9%), protein metabolism (13.0%), and metabolism and energy pathways (6.5%). In addition, other protein functional groups were related to regulation and nucleic acid metabolism (4.3%), immune response (4.3%), and transport (2.2%). Some proteins were not characterized by the database or had an unknown function (8.7%).

Proteins in enamel and dentin were also investigated through the protocol described for DEJ + EOM tissues. We were able to detect 207 proteins in dentin samples and 49 proteins in enamel samples (Tables S2 and S3). There were 15 proteins detected in all tissues (DEJ + EOM, enamel, and dentin). These proteins were primarily collagens. Moreover, in this study we observed 15 other proteins [isoform 3 of collagen alpha-1(II) chain (COL2A1), suprabasin isoform 1 precursor (SBSN), desmoglein-1 (DSG1), cystatin-A (CSTA), calmodulin-like protein 3 (CALML3), polyubiquitin-C (UBC), caspase-14 (CASP14), galectin-7 (LGALS7B), isoform 1 of transcriptional regulator ATRX (ATRX), isoform 3 of collagen alpha-1(XXII) chain (COL22A1), thioredoxin (TXN), two isoforms of AMELX (isoforms 1 and 3 of amelogenin, X isoform), prothrombin (fragment) (F2), and isoform 1 of peroxisomal proliferator-activated receptor A-interacting complex 285 kDa protein (PRIC285)] present solely in DEJ + EOM samples. These proteins were not detected in the enamel and dentin (Fig. 2).

Discussion

The DEJ and surrounding areas have been studied using many different physical techniques or biochemical

Table 1

Proteins detected by mass spectroscopy in laser captured microdissections of dentin–enamel junction (DEJ) and enamel organic matrix (EOM) tissues

Accession UniProtKB	Protein symbol	Protein name	Found in dentin*	Found in enamel*	Found in DEJ + EOM method 1	Found in DEJ + EOM method 2	Mascot score† Trypsin	No. of peptides Trypsin	SC (%) Trypsin	Mascot score† Semitr.	No. of peptides Semitr.	SC (%) Semitr.
P02452	COL1A1	Collagen alpha-1(I) chain	Yes	Yes	Yes	Yes	21990.9	445	68.8	22920.4	476	71.4
P08123	COL1A2	Collagen alpha-2(I) chain	Yes	Yes	Yes	Yes	13567.8	222	74.8	13998.4	257	72.6
P02768	ALB	Isoform 1 of Serum albumin	Yes	Yes	Yes	Yes	1266.7	24	38.4	1446.8	26	41.4
Q9NZT1	CALML5	Calmodulin-like protein 5	No	Yes	Yes	Yes	966.0	12	72.6	919.8	13	72.6
P15924	DSP	Isoform DPI of Desmoplakin	Yes	No	Yes	Yes	835.7	20	10.6	872.7	20	11.1
P02458	COL2A1	Isoform 3 of Collagen alpha-1(II) chain	No	No	No	Yes	804.3	2	13.8	913.4	5	15.6
Q86YZ3	HRNR	Hornerin	Yes	Yes	Yes	Yes	712.9	10	7.6	841.3	13	8.2
E9PBV3	SBSN	Suprabasin isoform 1 precursor	No	No	No	Yes	601.8	10	30.8	608.1	10	33.4
Q02413	DSG1	Desmoglein-1	No	No	Yes	Yes	452.8	7	12.2	492.2	8	13.8
P31151	S100A7	Protein S100-A7	Yes	Yes	Yes	Yes	359.8	5	35.6	349.5	5	35.6
P36955	SERPINF1	Pigment epithelium-derived factor	Yes	No	Yes	No	306.5	5	21.1	319.4	5	21.1
P21810	BGN	Biglycan	Yes	No	Yes	No	302.6	6	32.9	254.5	6	19.2
P14923	JUP	Junction plakoglobin	Yes	No	No	Yes	297.3	5	16.5	277.9	4	16.2
P01040	CSTA	Cystatin-A	No	No	No	Yes	296.0	5	87.3	317.9	5	80.6
P06702	S100A9	Protein S100-A9	Yes	Yes	Yes	Yes	252.4	5	59.6	350.7	6	60.5
Q5D862	FLG2	Filaggrin-2	Yes	Yes	Yes	Yes	250.8	4	2.7	288.0	4	3.6
P02765	AHSG	Alpha-2-HS-glycoprotein	Yes	Yes	Yes	No	247.6	5	12.2	357.4	7	20.7
P12273	PIP	Prolactin-inducible protein	Yes	Yes	No	Yes	232.4	5	56.8	215.7	4	46.6
P05109	S100A8	Protein S100-A8	Yes	Yes	No	Yes	213.6	4	47.3	249.5	4	47.3
P27482	CALML3	Calmodulin-like protein 3	No	No	No	Yes	210.4	3	41.6	211.4	3	30.9
P05997	COL5A2	Collagen alpha-2(V) chain	Yes	No	Yes	No	197.0	3	7.1	235.7	2	13.5
P04004	VTN	Vitronectin	Yes	Yes	Yes	No	188.1	3	7.1	189.6	3	7.1
P25311	AZGP1	Zinc-alpha-2-glycoprotein	Yes	No	Yes	Yes	183.0	4	21.1	176.3	4	21.1
P0CG48	UBC	Polyubiquitin-C	No	No	No	Yes	172.2	4	29.0	158.5	4	37.7
A2BF21	COL11A2	Collagen, type XI, alpha 2	Yes	No	Yes	No	162.2	3	3.2	401.6	4	10.7
P31944	CASP14	Caspase-14	No	No	No	Yes	161.7	3	25.2	192.0	4	29.3
Q6ZR08	DNAH12	Isoform 1 of Dynein heavy chain 12, axonemal	Yes	Yes	Yes	No	141.8	3	1.7			
P01042	KNG1	Isoform HMW of Kininogen-1	Yes	No	Yes	No	133.3	2	7.5	115.4	2	8.9
P47929	LGALS7B	Galectin-7	No	No	Yes	Yes	127.7	3	25.7	128.4	3	25.7
Q9NP70	AMBN	Isoform 2 of Ameloblastin	No	Yes	Yes	Yes	120.3	2	3.7	746.9	16	17.9
P04406	GAPDH	Glyceraldehyde-3-phosphate dehydrogenase	Yes	Yes	No	Yes	114.7	2	11.2	132.8	2	14.2
P10909	CLU	Clusterin	Yes	No	Yes	No	112.9	2	13.7			
P46100	ATRX	Isoform 1 of Transcriptional regulator ATRX	No	No	No	Yes	111.9	3	1.6			
Q8NFW1	COL22A1	Isoform 3 of Collagen alpha-1(XXII) chain	No	No	Yes	No	107.4	1	1.7	324.4	1	9.2
P10599	TXN	Thioredoxin	No	No	No	Yes	98.3	2	23.5			
Q15582	TGFBI	75 kDa protein	Yes	Yes	No	Yes	98.3	2	6.7	95.1	1	6.2
B4DF70	PRDX2	Peroxiredoxin-2	Yes	No	No	Yes	89.5	1	10.4	81.0	1	11.5
Q99983	OMD	Osteomodulin	Yes	No	Yes	No	87.5	2	9.5			
P04792	HSPB1	Heat shock protein beta-1	Yes	No	Yes	No	84.4	1	9.4			
P07355	ANXA2	Isoform 1 of Annexin A2	Yes	No	Yes	Yes	83.9	2	15.5	136.3	2	16.2

Table 1 Continued

Accession UniProtKB	Protein symbol	Protein name	Found in dentin*	Found in enamel*	Found in DEJ + EOM method 1	Found in DEJ + EOM method 2	Mascot score† Trypsin	No. of peptides Trypsin	SC (%) Trypsin	Mascot score† Semitr.	No. of peptides Semitr.	SC (%) Semitr.
P02461	COL3A1	Isoform 1 of Collagen alpha-1(III) chain	Yes	Yes	Yes	No				650.4	4	14.7
Q99217	AMELX	Isoform 3 of Amelogenin, X isoform	No	No	Yes	Yes				468.2	7	21.0
Q99217	AMELX	Isoform 1 of Amelogenin, X isoform	No	No	Yes	No				210.4	1	15.2
Q7Z6Z7	HUWE1	Isoform 2 of E3 ubiquitin-protein ligase HUWE1	Yes	No	Yes	No				166.4	2	1.5
Q9BYK8	PRIC285	Isoform 1 of Peroxisomal proliferator-activated receptor A-interacting complex 285 kDa protein	No	No	No	Yes				105.1	2	1.1
P00734	F2	Prothrombin (Fragment)	No	No	Yes	No				80.5	1	5.7

*Proteins found in this study.
†Proteins appear in descending order of their MASCOT score.
SC, sequence coverage; Semitr., semitrypsin.

Fig. 2. Proportional Venn diagrams showing the distribution of 236 total proteins identified in dentin–enamel junction + enamel organic matrix (DEJ + EOM), enamel, and dentin.

approaches. Thus, high-resolution electron microscopy was used to investigate the relationship between human enamel and dentin crystals at the DEJ (24). Raman microelectroscopy was used to study changes in the mechanical properties and chemical composition of DEJ in irradiated teeth (25). The use of scanning electron microscopy enabled discovery of a novel organic protein containing enamel matrix with 100–400 μm thickness, which extended from the DEJ into the cuspal enamel (13). Similarly, in the crowns of human teeth, a 200- to 300-μm zone of resilient (less mineralized and elastic) dentin has been found beneath enamel in DEJ using scanning electron microscopy (26). The biologic characteristics of the DEJ layer were also comprehensively studied using light-microscopy immunohistochemistry and also by immunoelectron microscopy (27). The DEJ region is an area of high local concentration of enzymes (matrix metalloproteinases and their inhibitors) that are involved in the degradation of extracellular matrix components. Also, growth factors and their binding proteins are stored in this region. The DEJ region may be involved in tissue metabolism, allowing selective cleavage of matrix components by proteases, thus liberating and activating the stored growth factors and generating potentially bioactive fragments that may exert their effects at a location some distance from the DEJ (27).

It is a fact that all the previously mentioned methods and techniques used for DEJ investigations are only indirect. It is not possible to directly isolate and pick up distinct and well-defined cells or tissue areas from teeth, which would facilitate their further proteomic analysis. The repertory of methods and tools for specific analyses of tissue-bound cell populations was considerably enriched by the introduction of LCM (28). The principles of LCM predetermines this method to be successfully used in dental proteomics. It is used for isolation of small pieces of cells and tissues, often mineralized, and for further proteomic study of these

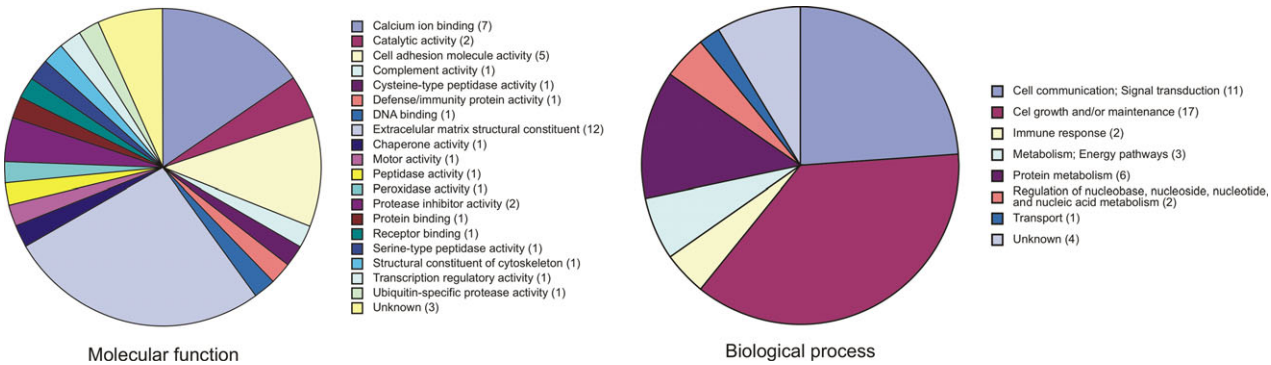

Fig. 3. Distribution of molecular functions and biological processes of proteins found in the dentin-enamel junction. The functions of proteins were categorized according to the classification system used in the public database (http://www.hprd.org).

samples. In this way, LCM – together with the LC-MS/MS technique – was successfully used to study proteins associated with dental cementum formation in mouse teeth (29). Laser capture microdissection was also utilized in comprehensive analyses of gene expression in mouse junctional epithelium and oral gingival epithelium to search for specific genetic markers of junctional epithelium, which attaches to tooth enamel at the dentogingival junction (30). Another study used the LCM technique to perform microdissection and isolation of selected regions of untreated mineralized bovine dentin (31).

The DEJ and EOM protein composition has previously been studied using different techniques, varying from immunofluorescent confocal microscopy (32), scanning electron microscopy, and confocal Raman spectroscopy (13) to gel electrophoresis associated with immunoblotting and mass spectrometry identification (33, 34). Proteins identified in DEJ and EOM using these techniques are discussed later in this section.

The use of LCM enabled us to study small areas of interest, such as the DEJ layer with the surrounding EOM, which have microscale dimensions. In combination with highly effective MS/MS techniques, we were able to investigate the proteomic composition of this highly mineralized layer with unique features, which still remains underestimated.

We applied two independent methods of extraction to isolate proteins from the highly mineralized tissues. Method 1 was based on direct protein digestion with trypsin followed by boiling the sample to denature proteins and repeating this step to obtain a higher yield of peptides and proteins. This method is simple and suitable for small LCM samples. Method 2 was somewhat different: heating the sample in trifluoroacetic acid caused effective demineralization sufficient to allow protein extraction; proteins were then reduced, alkylated, and cleaved by trypsin (16). It was of additional benefit that additional peptides could be revealed using Method 2. Combining the results obtained from these two methods enabled us to identify a total of 46 proteins in DEJ + EOM samples (Table 1). We also tried another protein-extraction method –extraction of proteins to 8 M urea solution (29). However, this method afforded a significantly lower yield in protein numbers (data not shown).

Database searching using two different enzyme search parameters (trypsin vs. semitrypsin) extended the total number of proteins and peptides detected. Using trypsin and semitrypsin as enzyme parameters enabled us to detect 40 and 41 proteins, respectively, and in combination, a total of 46 proteins were detected (Table 1).

No statistically important differences in protein composition in individual samples were observed, probably because of the small number of teeth used in this study.

The number of proteins found in DEJ + EOM samples represent the most extensive list of human DEJ + EOM proteins presented so far. Figure 3 displays pie charts of all the proteins identified from all the experiments. The molecular functions of these proteins are very broad and include calcium ion binding [isoform 1 of annexin A2 (ANXA2), CALML3, calmodulin-like protein 5 (CALML5), filaggrin-2 (FLG2), proteins S100-A7, -A8, and -A9 (S100A7, S100A8, and S100A9, respectively)], cell adhesion molecule activity [zinc-alpha-2-glycoprotein (AZGP1), DSG1, junction plakoglobin (JUP), LGALS7B, osteomodulin (OMD)], formation of the extracellular matrix [isoform 2 of ameloblastin (AMBN), AMELX (isoforms 1 and 3), biglycan (BGN), collagen alpha-1(I) chain (COL1A1), collagen alpha-2(I) chain (COL1A2), COL2A1, isoform 1 of collagen alpha-1(III) chain (COL3A1), collagen alpha-2(V) chain (COL5A2), collagen, type XI, alpha 2 (COL11A2), isoform 3 of collagen alpha-1(XXII) chain (COL22A1), and vitronectin (VTN)], protease inhibitor activity [cystatin-A (CSTA), isoform HMW of kininogen-1 (KNG1)] catalytic activity [TXN, glyceraldehyde-3-phosphate dehydrogenase (GAPDH)], and proteins with unknown functions [hornerin (HRNR), PRIC285, suprabasin isoform 1 precursor (SBSN)]. As expected, the biological processes in which proteins from mineralized tissues are involved are mainly cell growth and/or maintenance [AMBN, AMELX (isoforms 1 and 3), BGN, COL1A1, COL1A2, COL2A1, COL3A1, COL5A2, COL11A2, COL22A1, isoform 1 of dynein heavy chain 12, axonemal (DNAH12), DSG1, isoform DPI of desmoplakin

(DSP), LGALS7B, OMD, VTN), cell communication/signal transduction [alpha-2-HS-glycoprotein (AHSG), ANXA2), CALML3, CALML5, FLG2, JUP, S100A7, pigment epithelium-derived factor (SERPINF1), S100A8, S100A9, 75 kDa protein (TGFBI)], and protein metabolism [CASP14, CSTA, F2, heat shock protein beta-1 (HSPB1), KNG1, UBC] (Fig. 3). These findings demonstrate the ability of the methodology used in this work to investigate simultaneously a large number of proteins.

The DEJ region represents an area of biological activity resulting from the presence of a high local concentration of enzymes involved in the degradation of extracellular matrix components, in combination with the storage of growth factors and their binding proteins in this region. They may be involved in tissue metabolism by allowing selective cleavage of matrix components by the proteases, thus liberating and activating the stored growth factors and generating potentially bioactive fragments that may exert their effects at a location somewhat distant from the DEJ (27).

The DEJ is a protein-rich, fibril-reinforced bond, which is mineralized to a moderate degree. We have observed that the DEJ is rich in collagen type I (COL1A1 and COL1A2). Collagens type I are among the most abundant proteins in humans (35). They have also been detected in various human teeth tissues, such as dentin, tooth pulp, or dental cementum (4, 5, 36). Other types of collagen (type III and V) are scarce but present (11). Also, collagen type IV was observed in the DEJ region (33). The EOM associated with the DEJ revealed enrichment of collagen type VII and matrix metalloproteinase-20 (MMP-20) (32, 34). We have also detected the presence of collagen type II (COL2A1), collagen type III (COL3A1), collagen type V (COL5A2), collagen type XI (COL11A2), and even the quite rare collagen type XXII (COL22A1). Deposition of crystallites occurs within the collagen gap regions, along the collagen fibril network, leading to bridging of inter-collagen spaces. The nucleation and growth of crystals are promoted and developed with the help of a series of non-collagenous proteins, namely, phosphorylated proteins (e.g. dentin sialoprotein and dentin phosphoprotein), which play crucial roles in the mineralization process during tooth formation and DEJ formation (11).

The functionally largest group of proteins identified in this study was a group of proteins responsible for cell growth and/or maintenance (all collagens identified in this study, DSP, DSG1, BGN, DNAH12, LGALS7B, AMBN, OMD, and AMELX). The second largest group of proteins comprises proteins involved in cell communication and signal transduction (CALML5, S100A7, SERPINF1, JUP, CSTA, S100A9, FLG2, AHSG, S100A8, CALML3, TGFBI, and ANXA2). These findings provide information about the protein composition of the DEJ layer. The identified proteins are responsible for the unique functional and mechanical features of the DEJ layer joining two different tissues (enamel and dentin).

We have reported a group of 15 proteins, which were exclusively detected in the DEJ + EOM samples and were not detected in enamel or dentin (Table 1). However, 10 of these proteins (COL2A1, SBSN, DSG1, CALML3, CASP14, LGALS7B, TXN, two isoforms of AMELX, and F2) were observed in enamel or dentin in previous studies (1, 4). The remaining five proteins (COL22A1, CSTA, UBC, ATRX, and PRIC285) were previously detected in various parts of the body of humans or animals by other researchers but were not detected in dental tissues. Hence, some of these proteins are further discussed with respect to their possible functions in the DEJ layer.

Cystatins are thiol proteinase inhibitors, present ubiquitously in living organisms, including humans. Many studies have reported a variation in cystatin levels in different diseases, such as cancer, and it has been suggested that cystatins play a pivotal role in a variety of pathological conditions (37). The roles of cystatins in saliva have been investigated in several studies (38–40). Cystatin is an important saliva component. Several forms of cystatins (cystatin SA-III, cystatin SA, and cystatin SN) have been identified in whole saliva (40). Together with other saliva proteins, such as S100-A9 protein, statherin, and acidic proline-rich protein, cystatin strongly adsorbs to the tooth surface to form the acquired enamel pellicle (38). The acquired enamel pellicle is an oral, fluid-derived protein layer that protects teeth from enamel demineralization and abrasion. Individual, ethnic, and gender variations in the ability of salivary proteins to form pellicles under experimental conditions have been studied (39) and have revealed differences in the protective effects between healthy young Scandinavians and young non-Scandinavians. Slightly more of the SN-isoform of S-type cystatin was found in pooled parotid saliva from non-Scandinavian subjects showing highest protection of teeth. Cystatins in acquired enamel pellicle could play an important role in individual susceptibility to dental caries (41, 42). Exposure of tooth surfaces to acids causes enamel demineralization, which may lead to development of dental carious or non-carious lesions. The whole of saliva contains protective agents. Changes in the saliva proteome profile of human volunteers after exposure to acids were studied (41) and an increased abundance was observed of some proteins in acquired enamel pellicle. Among them, cystatin B was increased 20- and 13-fold after exposure to citric and lactic acid, respectively (41). Analysis of the composition of saliva and in vitro acquired enamel pellicle revealed a statistically significant correlation between the quantity of cystatin SN, and cystatin S (together with lipocalin and acidic proline-rich proteins) in samples from the caries-free group of subjects in comparison with the caries-susceptible group (42). There is no evidence in the literature for the presence of CSTA in enamel or dentin and its expression by ameloblasts or odontoblasts. Our observation of CSTA in the DEJ + EOM region is therefore surprising. The role of CSTA in this tissue remains unknown and is worthy of further investigation.

Collagen type XXII is a member of fibril-associated collagens. It is a specific component of tissue junctions

as this extracellular matrix protein is present only at tissue junctions (43). It is predominantly found in the heart and skeletal muscle of human tissue and to a lesser extent in cartilage and skin in mice. It has been identified in specific tissue junctions, namely the myotendinous junctions that present the major site of muscle force transmission to tendons (44). The role of collagen type XXII in the DEJ and/or EOM is unknown but it can be anticipated that its function in the DEJ might be similar to that exerted in other specific tissue junctions.

The importance of the DEJ for the correct function of the tooth and enamel entity during mastication of food can be demonstrated in patients undergoing radiotherapy. Patients with oral cancer are often subjected to radiotherapy, and an observed adverse effect of this procedure is increased susceptibility to oral diseases with dental lesions differing in location, appearance, and progression. The process may be initiated by an enamel shear fracture and continue to deeper parts of the tooth (45). McGuire *et al*. (46) demonstrated a direct link between radiation and dentition breakdown and a significant correlation of tooth-level radiation dose with the severity of individual tooth breakdown. Radiotherapy can cause total delamination of enamel from dentine. Simulated radiotherapy produced an increase in the stiffness of enamel and dentine near the DEJ. Increased stiffness is speculated to be a result of the radiation-induced decrease in the protein content, with the percentage reduction much greater in enamel sites (25). McGuire *et al*. (46) compared teeth extracted from oral patients treated with radiotherapy with those extracted from a control group of healthy subjects. Changes in MMP-20 expression and activity were observed. Matrix metalloproteinase-20 is a radiation-resistant component of mature tooth crowns enriched in DEJ. McGuire *et al*. (46) deduced that MMP-20 catalyzed the degradation of organic matrix at the DEJ site, leading to enamel delamination associated with oral cancer radiotherapy. Another protein in the DEJ that is affected by high-dose radiotherapy is collagen type IV. Reduced level of this protein was observed after exposure to >60 Gray irradiation. Because collagen type IV forms a network structure and has a propensity to stabilize the dermal–epidermal junction, it can be proposed that lower abundance of collagen type IV in the DEJ after tooth irradiation can explain its lower fracture toughness, lower crack propagation resistance, and instability (33). Changes in the mechanical properties and chemical composition could potentially contribute to biomechanical failure of the DEJ, leading to enamel delamination that occurs in the post-radiotherapy phase.

Surprisingly, we did not find any MMP-20 or collagen type IV in the DEJ layer in this study, perhaps because of limitations of our methodological approach in comparison with more common proteomic approaches (gel electrophoresis analysis of proteins followed by western blotting). The techniques used in this study can sufficiently degrade proteins and render them hardly detectable by mass spectrometry, whereby they are not also suitable for western blotting or gel electrophoresis analysis. This also demonstrates the limits of the data obtained by combination of LCM and mass spectrometry, which provides only a partial view on the composition of enamel, dentin, and DEJ + EOM.

In conclusion, more work must be carried out to elucidate the functional roles of the proteins identified in this study in the unique DEJ layer and the adjacent EOM region. This might provide a better understanding of adverse radiotherapy-induced effects on tooth structure, and improved preventive and restorative treatments for oral cancer patients.

Acknowledgements – This work was supported by Czech Science Foundation (grant number 17-10832S), research program of Charles University Prague PROGRES Q29/1LF, and with support for long-term conceptual development of research organization RVO:67985823.

Conflicts of interest – All authors declare that there are no potential conflicts of interest.

References

1. Castiblanco GA, Rutishauser D, Ilag LL, Martignon S, Castellanos JE, Mejía W. Identification of proteins from human permanent erupted enamel. *Eur J Oral Sci* 2015; **123**: 390–395.
2. Smith C. Cellular and chemical events during enamel maturation. *Crit Rev Oral Biol Med* 1998; **9**: 128–161.
3. Moranian-Oldak J. Protein-mediated enamel mineralization. *Front Biosci* 2012; **17**: 996–2023.
4. Jágr M, Eckhardt A, Pataridis S, Mikšík I. Comprehensive proteomic analysis of human dentin. *Eur J Oral Sci* 2012; **120**: 259–268.
5. Eckhardt A, Jágr M, Pataridis S, Mikšík I. Proteomic analysis of human tooth pulp: proteomics of human tooth. *J Endod* 2014; **40**: 1961–1966.
6. Linde A. Dentin matrix proteins, composition and possible functions in calcification. *Anat Rec* 1989; **224**: 154–166.
7. Jágr M, Eckhardt A, Pataridis S, Broukal Z, Dušková J, Mikšík I. Proteomics of human teeth and saliva. *Physiol Res* 2014; **63**(Suppl): 141S–154S.
8. Lin CP, Douglas WH. Structure-property relations and crack resistance at the bovine dentin-enamel junction. *J Dent Res* 1994; **73**: 1072–1078.
9. Arsenault AL, Robinson BW. The dentino-enamel junction: a structural and microanalytical study of early mineralization. *Calcif Tissue Int* 1989; **45**: 111–121.
10. White SN, Paine ML, Luo W, Sarikaya M, Fong H, Yu Z, Li ZC, Snead ML. The dentino-enamel junction is a broad transitional zone uniting dissimilar bioceramic composites. *J Am Ceram Soc* 2000; **83**: 238–240.
11. Goldberg M. The dentinoenamel junction. In: Goldberg M, ed. *Understanding dental caries: from pathogenesis to prevention and therapy*. Switzerland: Springer International Publishing, 2016; 75–83.
12. Paine M, White S, Luo W, Fong H, Sarikaya M, Snead M. Regulated gene expression dictates enamel structure and tooth function. *Matrix Biol* 2001; **20**: 273–292.
13. Dusevich V, Xu C, Wang Y, Walker MP, Gorski JP. Identification of a protein-containing enamel matrix layer which bridges with the dentine-enamel junction of adult human teeth. *Arch Oral Biol* 2012; **57**: 1585–1594.
14. Myoung S, Lee J, Constantino P, Lucas P, Chai H, Lawn B. Morphology and fracture of enamel. *J Biomech* 2009; **42**: 1947–1951.
15. Mikšík I, Ergang P, Pácha J. Proteomic analysis of chicken eggshell cuticle membrane layer. *Anal Bioanal Chem* 2014; **406**: 7633–7640.

16. Roulhac PL, Ward JM, Thompson JW, Soderblom EJ, Silva M, Moseley MA, Jarvis ED. Microproteomics: quantitative proteomic profiling of small numbers of laser-captured cells. *Cold Spring Harb Protoc* 2011; **2011**: pdb.prot5573.
17. Shapiro JP, Biswas S, Merchant AS, Satoskar A, Taslim C, Lin S, Rovin BH, Sen CK, Roy S, Freitas MA. A quantitative proteomic workflow for characterization of frozen clinical biopsies: laser capture microdissection coupled with label-free mass spectrometry. *J Proteomics* 2012; **77**: 433–440.
18. Kouznetsova I, Gerlach KL, Zahl C, Hoffmann W. Expression analysis of human salivary glands by laser microdissection: differences between submandibular and labial glands. *Cell Physiol Biochem* 2010; **26**: 375–382.
19. Sun JX, Horst OV, Bumgarner R, Lakely B, Somerman MJ, Zhang H. Laser capture microdissection enables cellular and molecular studies of tooth root development. *Int J Oral Sci* 2012; **4**: 7–13.
20. Thennavan A, Sharma M, Chandrashekar C, Hunter K, Radhakrishnan R. Exploring the potential of laser capture microdissection technology in integrated oral biosciences. *Oral Dis* 2016; **23**: 737–748.
21. Rappsilber J, Mann M, Ishihama Y. Protocol for micro-purification, enrichment, pre-fractionation and storage of peptides for proteomics using Stage Tips. *Nat Protoc* 2007; **2**: 1896–1906.
22. Ošťádal M, Eckhardt A, Herget J, Mikšík I, Dungl P, Chomiak J, Frydrychová M, Burian M. Proteomic analysis of the extracellular matrix in idiopathic pes equinovarus. *Mol Cell Biochem* 2015; **401**: 133–139.
23. Jágr M, Eckhardt A, Pataridis S, Foltán R, Myšák J, Mikšík I. Proteomic analysis of human tooth pulp proteomes – Comparison of caries-resistant and caries-susceptible persons. *J Proteomics* 2016; **145**: 127–136.
24. Bodier-Houllé P, Steuer P, Meyer JM, Bigeard L, Cuisinier FJG. High-resolution electron-microscopic study of the relationship between human enamel and dentin crystals at the dentinoenamel junction. *Cell Tissue Res* 2000; **301**: 389–395.
25. Reed R, Xu C, Liu Y, Gorski JP, Wang Y, Walker MP. Radiotherapy effect on nano-mechanical properties and chemical composition of enamel and dentine. *Arch Oral Biol* 2015; **60**: 690–697.
26. Zaslansky P, Friesem AA, Weiner A. Structure and mechanical properties of the soft zone separating bulk dentin and enamel in crowns of human teeth: insight into tooth function. *J Struct Biol* 2006; **153**: 188–199.
27. Goldberg M, Septier D, Bourd K, Hall R, Jeanny J-C, Jonet L, Colin S, Tager F, Chaussain-Miller C, Garabédian M, George A, Goldberg H, Menashi S. The dentino-enamel junction revisited. *Connect Tissue Res* 2002; **43**: 482–489.
28. Emmert-Buck MR, Bonner RF, Smith PD, Chuaqui RF, Zhuang Z, Goldstein SR, Weiss RA, Liotta LA. Laser capture microdissection. *Science* 1996; **274**: 998–1001.
29. Salmon CR, Giorgetti AP, Leme AFP, Domingues RR, Sallum EA, Alves MC, Kolli TN, Foster BL, Nociti FH Jr. Global proteome prifiling of dental cementum under experimentally-induced apposition. *J Proteomics* 2016; **141**: 12–23.
30. Hayashi Y, Matsunaga T, Yamamoto G, Nishii K, Usui M, Yamamoto M, Tachikawa T. Comprehensive analysis of gene expression in the junctional epithelium by laser microdissection and microarray analysis. *J Periodontal Res* 2010; **45**: 618–625.
31. Dorvee JR, Deymier-Black A, Gerkowicz L, Veis A. Peritubular dentin, a highly mineralized, non-collagenous, component of dentin: isolation and capture by laser microdissection. *Connect Tissue Res* 2014; **55**(S1): 9–14.
32. McGuire JD, Walker MP, Mousa A, Wang Y, Gorski JP. Type VII collagen is enriched in the enamel organic matrix associated with the dentin-enamel junction of mature human teeth. *Bone* 2014; **63**: 29–35.
33. McGuire JD, Gorski JP, Dusevich V, Wang Y, Walker MP. Type IV collagen is a novel DEJ biomarker that is reduced by radiotherapy. *J Dent Res* 2014; **93**: 1028–1034.
34. McGuire JD, Walker MP, Dusevich V, Wang Y, Gorski JP. Enamel organic matrix: potential structural role in enamel and relationship to residual basement membrane constituents at the dentin enamel junction. *Connect Tissue Res* 2014; **55** (S1): 33–37.
35. Prockop DJ, Kivirikko KI. Collagens: molecular biology, diseases, and potentials for therapy. *Annu Rev Biochem* 1995; **64**: 403–434.
36. Salmon CR, Giorgetti APO, Paes Leme AF, Domingues RR, Kolli TN, Foster BL, Nociti Jr FH. Microproteome of dentoalveolar tissues. *Bone* 2017; **101**: 219–229.
37. Shamsi A, Bano B. Journey of cystatins from being mere thiol protease inhibitors to a heart of many pathological conditions. *Int J Biol Macromol* 2017; **102**: 674–693.
38. Heller D, Helmenhorst EJ, Oppenheim FG. Saliva and serum protein exchange at the tooth enamel surface. *J Dent Res* 2017; **96**: 437–443.
39. Bruvo M, Moe D, Kirkeby S, Vorum H, Bardow A. Individual variations in protective effects of experimentally formed salivary pellicles. *Caries Res* 2009; **43**: 163–170.
40. Yao Y, Berg EA, Costello CE, Troxler RF, Oppenheim FG. Identification of protein components in human acquired enamel pellicle and whole saliva using novel proteomics approaches. *J Biol Chem* 2003; **278**: 5300–5308.
41. Delecrode TR, Siqueira WL, Zaidan FC, Bellini MR, Moffa EB, Mussi MCM, Xiao Y, Buzalaf MAR. Identification of acid-resistant proteins in acquired enamel pellicle. *J Dent* 2015; **43**: 1470–1475.
42. Vitorino R, De Morais GS, Ferreira R, Lobo MJC, Duarte J, Ferrer-Correia AJ, Tomer KB, Domingues PM, Amado FML. Two-dimensional electrophoresis study of in vitro pellicle formation and dental caries susceptibility. *Eur J Oral Sci* 2006; **114**: 147–153.
43. Koch M, Schulze J, Hansen U, Ashwodt T, Keene DR, Brunken WJ, Burgeson RE, Bruckner P, Bruckner-Tuderman L. A novel marker of tissue junctions, collagen XXII. *J Biol Chem* 2004; **279**: 22514–22521.
44. Kehlet SN, Karsdal MA. Type XXII collagen. In: Karsdal MA, ed. *Biochemistry of Collagens, Laminins and Elastin: Structure, Function and Biomarkers*. Herlev, Denmark: Nordic Science, 2016; 135–137.
45. Vissink A, Burlage FR, Spijkervet FKL, Jansma J, Coppes RP. Prevention and treatment of the consequences of head and neck radiotherapy. *Crit Rev Oral Biol Med* 2003; **14**: 213–225.
46. McGuire JD, Mousa AA, Zhang BJ, Todoki LS, Huffman NT, Chandrababu KB, Moradian-Oldak J, Keightley A, Wang Y, Walker MP, Gorski JP. Extracts of irradiated mature human tooth crowns contain MMP-20 protein and activity. *J Dent* 2014; **42**: 626–635.

Supporting Information

Additional Supporting Information may be found in the online version of this article:

Table S1. The list of proteins and their peptide sequences identified exclusively by mass spectrometry in DEJ+EOM tissues.

Table S2. Proteins detected by mass spectroscopy in laser captured microdissections of dentin tissues

Table S3. Proteins detected by mass spectroscopy in laser captured microdissections of enamel tissues